

# We are IntechOpen, the world's leading publisher of Open Access books Built by scientists, for scientists

6,900

Open access books available

186,000

International authors and editors

200M

Downloads

Our authors are among the

154

Countries delivered to

TOP 1%

most cited scientists

12.2%

Contributors from top 500 universities



WEB OF SCIENCE™

Selection of our books indexed in the Book Citation Index  
in Web of Science™ Core Collection (BKCI)

Interested in publishing with us?  
Contact [book.department@intechopen.com](mailto:book.department@intechopen.com)

Numbers displayed above are based on latest data collected.  
For more information visit [www.intechopen.com](http://www.intechopen.com)



---

# High-Temperature Oxidation of Metals

---

Sneha Samal

Additional information is available at the end of the chapter

<http://dx.doi.org/10.5772/63000>

---

## Abstract

This chapter explains the brief understanding of the high-temperature oxidation of pure metals such as iron, copper and zinc. Effect of crystal structure from fcc to bcc and hcp on the role of high-temperature oxidation is described briefly. Simultaneously, the effect of grain size of these metals and grain boundary displacement during oxidation process are described very clearly. The combined effect of crystal structure and grain size on the formation of oxide scale is studied in depth understanding with support from the literature search. The aim of this chapter is to explain the mechanism and experimental evidence for the high-temperature oxidation of pure metals.

**Keywords:** oxidation, pure metal, high temperature, crystal structure, grain size

---

## 1. Introduction

Generally, most of the metals used in common application technologies undergo deterioration on exposure to weather condition with time. Consequently, most of the metals are subject to corrosion either at room temperature or at high-temperature ranges [1]. High-temperature corrosion issues deal with energy conversion by turbines, nuclear power, solid oxide fuel cells and high-temperature thermoelectric system [2]. In conventional coal-fired power plants, combustion process is used to heat water to produce steam and that powers turbine to generate electricity. The fireside and steam side of chromia-forming ferritic steels used for the heater tubes face problems of high-corrosion system [3]. The increased temperature and high-steam contents will result in rapid material degradation, and there is a need for high-temperature alloys. The gas-fired turbines at high temperature are limited due to rapid diffusion and oxidation rates. The investigation is carried out for high-temperature materials to increase efficiencies and lower emissions. Similarly, nuclear power plants use fossil for generation of thermal energy that

is used in heat-pressurized water [4]. The use of high-temperature materials and its behavior towards corrosion process are subject of interest. The metallic materials used in nuclear metallic materials face the corrosion such as stress corrosion cracking (SCC), irradiation-assisted cracking corrosion (IASCC), environmentally assisted cracking (EAC) and intergranular cracking (IGA) [5]. The rate of corrosion varies widely from slower to faster degree depending on the type of material. The examples of such type are iron rusts at room temperature and deteriorate faster than nickel and chromium that are attacked slowly with time. The surface layer that results due to oxidation determines nature of corrosion rate on the metal and has a strong effect on the material [6].

The high-temperature oxidation of metals always attracts attention from the readers and researchers community as the enthusiastic subject of investigation. This area covers both theoretical predication and satisfactory subject of investigation based on the various combined areas such as metallurgical, chemical and physical discipline with thermodynamic predication [7]. Recently, a set of mechanics data available on mass transport through oxide scales during oxidation, evaporation of oxide species, the role of mechanical stress on oxide scales and the important relationships between metal elements, microstructure and oxidation. Accordingly, such information is obtained virtually prior to oxidation to obtain the physical and chemical reaction of metal species at high temperature [8].

The understanding of the oxidation phenomena and the mechanism behind the reaction species for the formation of oxide scales and its role for the formation of various layers of oxide scale on the metal were discussed. The role of crystal structure of pure metals plays the viable role in the formation of oxide scale [9]. Effect of grain boundary determines the formation of oxide scale and rate of oxidation during high-temperature oxidation scale [10]. The main purpose of the chapter is an introduction to fundamental as well as experimental investigation of interaction of reactive species such as oxygen as the component usually metals such as high temperature. The rate of corrosion depends on the nature of reaction products. The rate of reaction is controlled by reactants through the solid layers. The rate of formation of oxide layers on metals is accordingly [11]



The extent of reaction determines the amount of metal consumed, the amount of oxygen used and the amount of product formed during oxidation process. There are several rate laws that apply to determine the oxidation rates such as linear, parabolic and logarithmic rates. The linear law is based on the surface reaction step towards the reactive gases of the environment. It is independent of the time of the reaction. However, the parabolic law depends on inversely proportional to square root of time and is obeyed when diffusion through scale is rate determining steps [12]. The logarithmic law is applicable to the very thin oxide films in the range of 2–4 nm [13].

Discontinuous method is the way to measure the weight of the sample within an interval of the time on exposure to high temperature. Every interval of certain time samples needs to be

removed from the high-temperature reactive zone removed the oxide scales from the surface and weighed effectively [14]. Assessment of the extent of reaction is carried out in a simple way either by observing the mass gain of the oxidized samples that is the mass of oxygen taken into scale or by observing the mass loss of the base sample which is equivalent to the mass gain by the oxide scale. The change in specimen dimension is also observed during high-temperature oxidation. The disadvantage of this method is the many specimens are needed to study the reaction kinetics and progress of the reaction is not continuous [12]. On the other hand, this method was very simple and the apparatus required is very simple. Also at each individual point, metallographic examination of each data point is evaluated.

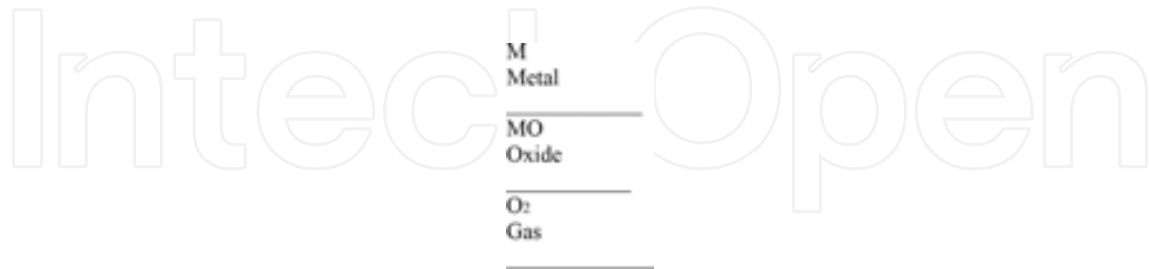
There are various ways to examine and analyze the surface of oxidized samples from the scale towards the base of the material. The methods are classified into two broad categories: (i) from the basic sample mounting to preparation and (ii) then examination using various techniques towards the final stage. Generally, the samples were mounted on the epoxy resin, and then polished using diamond grinding to observe the samples' microstructures and scale thickness and ion transportation from scale towards base of the pure metal. As the epoxy method is very easy, simple and convenient way to examine the scale and the base of the sample. The polished specimens may be examined using conventional optical microscopy for the microstructures, and the elements analyzed can be carried out using scanning electron microscope. Etching is followed on samples after metallographic preparations. Optical microscope is the simplest technique available to look the optical images of the metals before and after oxidation. To know better in microstructure and element of oxides present in oxidized scale and also migration of ions towards base, scanning electron microscopy with energy dispersive X-ray is the best way to know all the experimental parameters that control the oxidation rate of the material [13]. The specific band energy and band states also can be determined on oxidized scales and base of the materials. X-ray diffraction techniques also can be used to determine the corresponding phases of oxide group on the oxidized scale of the pure metal [14]. A depth understanding of high-temperature corrosion of pure metals is quite necessary as the alloys in multicomponent form makes the reaction process more complex in nature. The sample like pure metal is the beginning stage and simplest way of understanding the reaction kinetics and nature of reaction during high temperature in gaseous phase. The role of temperature and duration of oxidation play the crucial role in formation of oxide layers on the surface of pure metals.

## 2. Mechanism of oxidation

Transport mechanism of ions and electrons during the oxidation of pure metals is well explained by Wagner's theory of oxidation [15]. According to Wagner's theory, oxidation rate is controlled by partial ionic and electronic conductivities of oxides and their dependence on the chemical potential of the metal or oxygen in the oxide. According to Kofstad [16], the defect structure of oxides plays the important role in oxidation rate of metal. The consideration of the reaction is



It is obvious that the solid reaction product MO will separate the two reactants as shown in **Scheme 1**.



**Scheme 1.** Metal (M) and reaction phase ( $O_2$ ) through oxide layer (MO).

In order to proceed the further reaction, one of the reactants either metal or gas ( $O_2$ ) must penetrate through the oxide scale interface to reach either site of the reactant species. This mechanism of penetration of reactants through oxide layer plays the important role in formation of sublayers in high-temperature oxidation process. Since all metal oxides are ionic in nature, the possibility of transport of neutral metal through the interface is not feasible. Transport of ions through ionic solid is well explained by several mechanisms that belong to the stoichiometric crystal structure or nonstoichiometric crystal one. There are two types of defects that predominate the mobility of ions such as Schottky and Frenkel defects concept [17]. In Schottky defects, ionic vacancies are transported by both the concentration of anionic and cationic sublattices. However, in Frenkel defects, ionic vacancies are transported mainly by cation vacancies. The cations are free to migrate any direction of cations or interstitial sites (**Figure 1**).

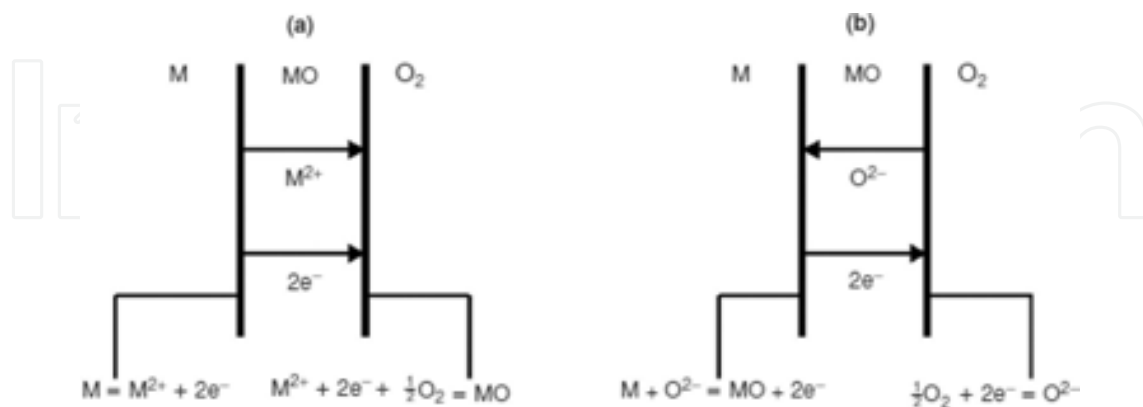


**Figure 1.** The ions are free movement of oxygen on lattice sites. Interfacial reactions and transport processes for high-temperature oxidation mechanisms (a, cation mobile; and b, anion mobile).

However, both of the reactions could not able to explain the transport mechanism during oxidation state because neither any of the defect structure provides the mechanism for

transport of electrons through the interface. In order to explain both migration of electrons and ions it has to be assumed that oxides that are formed during oxidation are nonstoichiometric compounds [18] (Figure 2).

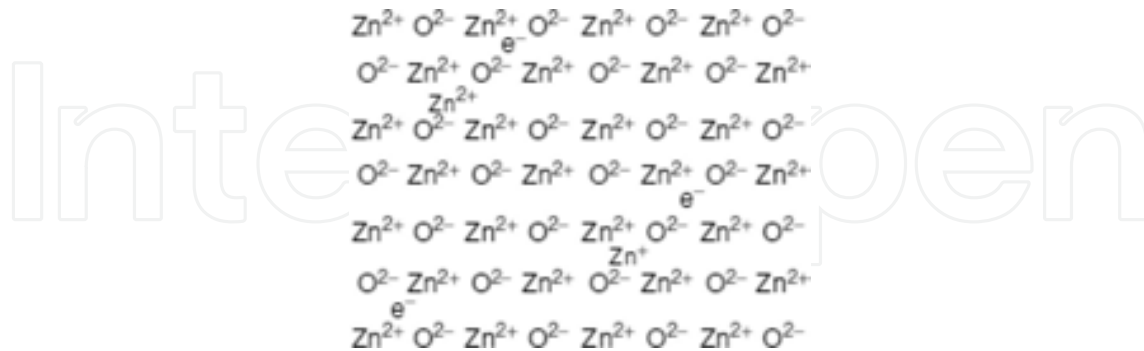


Figure 2. Interstitial cations and excess electrons in ZnO an n-type of metal excess semiconductor.

Nonstoichiometric ionic compounds are classified as semiconductors that may show some positive or negative behaviour. Zinc oxide is the best example of this type of structure. The electric charge is carried out by negative carriers either by metal deficit or metal excess [19].

### 2.1. Metal excess

The chemical formula for metal excess is M<sub>1+δ</sub>O, and the best example of it is ZnO. In order to allow extra metal in this compound it is necessary to create existence of interstitial cations with equivalent number of electrons in conduction band [20] (Figure 3).

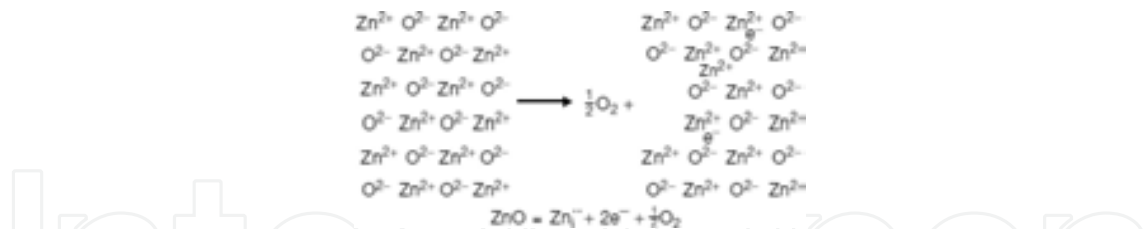


Figure 3. Formation of metal-excess ZnO with excess electrons and interstitial Zn ions from perfect ZnO.

In the above image, both Zn<sup>+</sup> and Zn<sup>2+</sup> can create possible space for interstitial sites. Cation conduction can occur over interstitial sites and electric conduction can occur by excess electrons excited into conduction site named as quasi-free electrons. The formation of defect in the ZnO crystal is represented as below [21]



The formation of Z $\ddot{n}_i$  is doubly charged Zn interstitial ions and can be written as



For the formation of  $Zn_i^\oplus$ , singly charged Zn interstitial ions enter the interstitial sites. The final equilibrium constant can be determined as follows

$$C_{Zn_i} = C_e \alpha PO_2^{-\frac{1}{4}} \tag{5}$$

This explains that defect structure has no role in the mechanism and shows that both the single- and double-charged interstitial cations have a significant role in the mechanism.

More recently, it has been reviewed that significant interstitial solution of zinc occurs in ZnO. Some other researcher also predicts the mechanism by neutral zinc atoms or single-charged interstitial ions. On the basis of oxygen diffusion, the vacancies can occur above by 1000°C. So still there is ambiguity about the mechanism and interpretation of ZnO [22]. Inconsistencies in different mechanisms may arise due to defect structures that are resulted from impurities of the samples especially. So the analysis of pure metal towards high-temperature investigation is a very essential step in concern.

Nonmetal deficit occurs on evaporation of oxygen ions from the species and the electrons enter the conduction band as a result it created vacancy as anion lattice (**Figure 4**). The process is represented as follows [23]

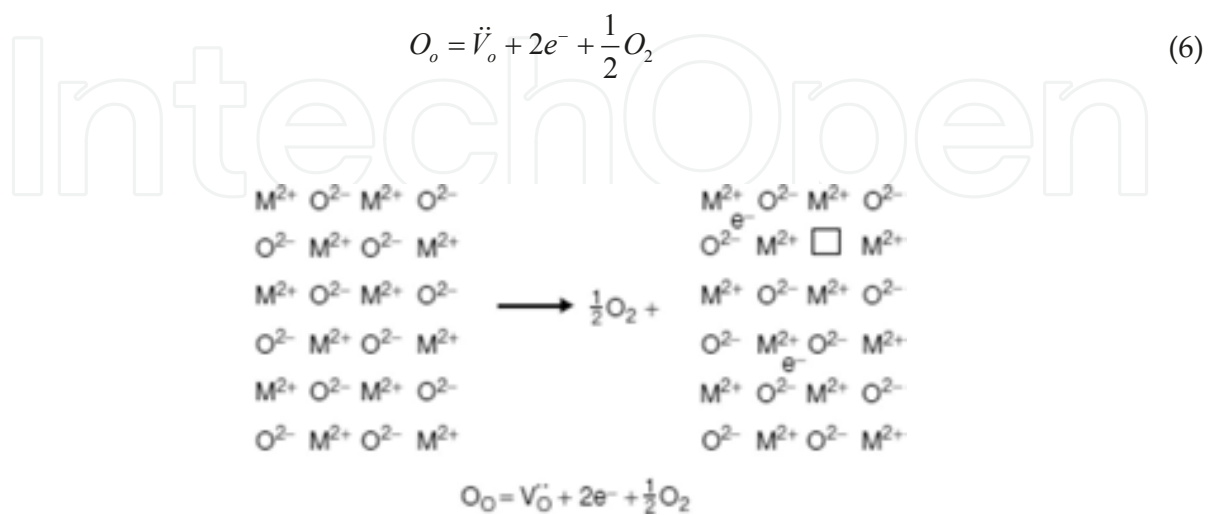


**Figure 4.** Formation of oxygen deficit MO with oxygen vacancies and excess electrons from perfect MO.

The vacant oxygen site is surrounded by the positive ions represent a site for high positive charge to which free electrons can be attracted. So there is possibility the following reaction takes place as follows



Therefore we have possibilities of single- and double-charged vacancies as well as neutral vacancies.

## 2.2. Intrinsic semiconductor

The oxide of CuO behaves in this way at 1000°C. This is quiet deviation from the general category. This material is the subject of interest for the study of high-temperature oxidation of metal. Also the lattice structure of Cu belongs to BCC type, which is one of the interesting points on considering various crystal structures into high-temperature oxides and evaluating its role of packing fraction in lattice structure towards the high-temperature oxidation of pure metals (Figure 5).

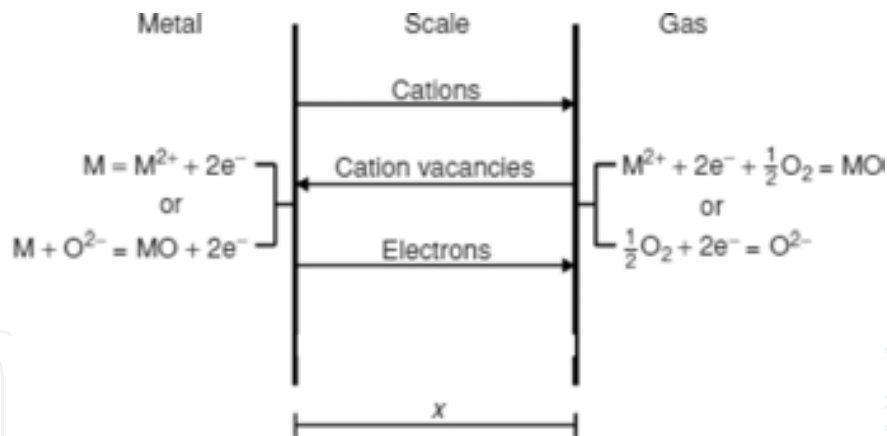


Figure 5. Simplified model for diffusion-controlled oxidation.

Rate of oxidation depends on how the oxidation process proceeds under those conditions where two reactants such as metal and oxygen are separated by an oxidized product. Ionic and electronic transport processes through oxide scale are accompanied by phase boundary reactions, and formation of new oxide species depends on whether cations or anions are transported through oxide layer. Thus the transport mechanisms of oxidation process are varied with oxygen pressure and temperature. Highest oxidation rate is observed in the metal sample where highest defect concentration is possible.

### 2.3. Point defect model

Point defect model refers to the movement of point defects in an associated electric field. Expansion behaviour of a passive film on a metal surface and breakdown of passive films in terms of mass and charge flux via purpose defects across the semiconductive and defective barrier layers of the passive film. Point defect model has allowed to formulate a set of principles for designing new alloys and has led to the development of a determine for predicting localized corrosion damage functions [24]. Passive film is the defective compound layer that results ion vacancies and chemical element vacancies that were generated and exterminated at the metal–film and film–solution interfaces. However, the bilayer structure of the film comprising a defective or binary compound barrier layer adjacent to the metal and an outer layer that forms by precipitation from reaction of cation species with surroundings introduced metal interstices to the defects in the barrier layer dissolution with passive current reside within the barrier.

### 2.4. Linear rate law

Under certain conditions, the oxidation of a metal proceeds at a constant rate and is said to obey the ‘linear rate law’.

$$x = klt \quad (9)$$

where  $x$  is the scale thickness and  $kl$  is the linear rate constant.

## 3. Oxidation of pure metals

### 3.1. Types of metals and crystal structure

Metals that have useful properties including strength, ductility, thermal and electrical conductivity are used in structural and electrical application. Understanding the structure of the metals can help us understand their properties. Metals are composed of atoms, and atoms are held by strong and delocalized bonds. These bonds are formed by a cloud of valence electrons that are shared by positive metal ions (cations) in a crystal lattice. An actual piece of metal consists of many tiny crystals called grains that join at the grain boundaries. The properties of the metals are influenced by the crystal structures, e.g., the face-centered cubic (fcc) structures. The atomic packing fraction in hcp ( $c/a = 1.633$ ) and fcc structure is 0.74 whereas the bcc crystal structure is less densely packed having atomic packing fraction of 0.68. Exposure of metals to high temperatures in air leads to oxidation of metals and to the formation of oxide scales. Oxidation of pure Fe having bcc is well documented and has led to the classical three layer scale characterization. At high temperatures above 570°C, the innermost layer with the lowest oxygen content is wustite (FeO), with an intermediate magnetite (Fe<sub>3</sub>O<sub>4</sub>) layer and the most oxygen-rich oxide hematite (Fe<sub>2</sub>O<sub>3</sub>) next to the gas phase. At temperature of 570°C diffusion transports phenomena occurs as a result, the wustite phase does not form and only

the magnetite and hematite layers are seen in scale and the rate of scaling is correspondingly low in the absence of wustite.

However the oxide scales formed in the case of copper (fcc) consist of an outer copper oxide layer and inner porous layer. The copper oxide may be single-phase CuO or a two-phase (CuO + Cu<sub>2</sub>O). At the lower part of the temperature range the oxidation kinetics and oxide morphology depend strongly upon the formation of CuO. The CuO layer is nonprotective and further oxidation Cu<sub>2</sub>O is converted to CuO. The formation of CuO changes the oxidation behavior from being approximately parabolic growth to having a break way like oxidation behavior. At ambient partial pressure of CuO, the oxide scale consists solely of Cu<sub>2</sub>O, while at higher oxygen pressures the scale consist of Cu<sub>2</sub>O (99%) + CuO and the rate constant is independent of oxygen pressure.

Zinc (hcp) forms ZnO and therefore a single phase, single-layered scale is expected when pure zinc is oxidized.

Also with addition to crystal structure, grain shape, size, and grain boundary diffusion on high temperature play the influential role on oxidation of pure metals. In this section we consider pure Cu, Fe and Zn at the subject of interest from the range of pure metals because of different crystal structures and the general application in industrial point of interest.

#### 4. Experimental conditions and reaction temperature

Three commercially pure metals such as iron, copper and zinc having different crystal structures were taken into consideration [27]. The specimens are cut in rectangular dimension of 50 × 25 × 6 mm<sup>3</sup>. The specimens are ground and polished up to 1 μm and subsequently etched to reveal the microstructure. The prepared specimens were examined using optical microscope for the microstructures of the preoxidized specimen. The specimens are further ground, polished and subsequently cleaned in acetone for oxidation species. The polished and cleaned specimens are placed in the central zone of the furnace for oxidation at dry air. In order to study the effect of crystal structures of metals, the samples are oxidized 2/3 of the melting point of metals. The oxidation tests are carried out for the period of 10 hours at temperatures of 1023°C, 723°C and 279°C for iron (bcc), copper (fcc) and zinc (hcp) metal, respectively [27]. The weight gain of the oxidized specimens was measured by means of an electronic microbalance with an accuracy of ±0.01 mg, and corrosion rates were calculated. The external scales of oxidized specimens were characterized by scanning electron microscope and energy dispersive spectroscopy.

#### 5. Results

The optical microstructure images of the preoxidized specimens of zinc, copper and iron are shown in **Figure 6**. The microstructure of zinc consists of coarse grains along with mechanical

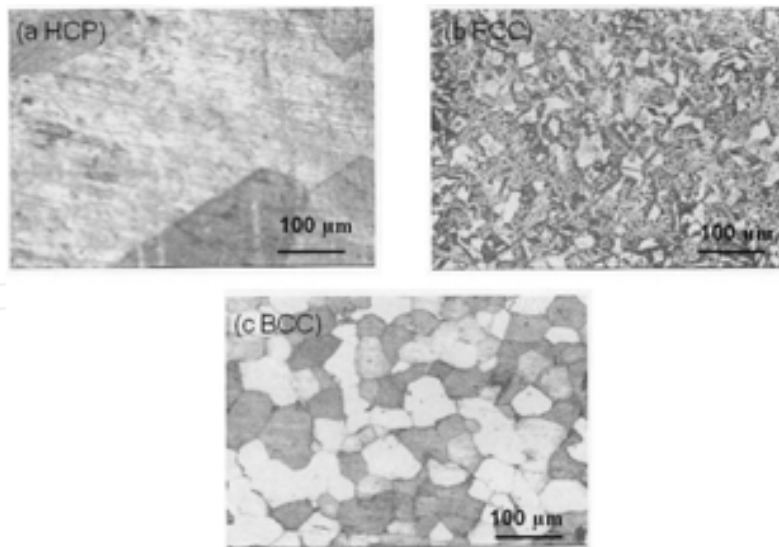


**Figure 6.** Optical micrographs of pure (a) Zn, (b) Cu and (c) Fe.

twins, whereas the microstructure of copper shows polyhedral grains with annealing twins. The microstructure of pure iron shows polyhedral grains of ferrite with very distinct and sharp boundaries. The oxidation rate of pure iron having bcc crystal structure is found to be  $13.37 \times 10^{-3} \text{ g cm}^{-2} \text{ h}^{-1}$ . However, the oxidation rates of copper and zinc are found to be  $0.69 \times 10^{-3} \text{ g cm}^{-2} \text{ h}^{-1}$  and  $0.05 \times 10^{-3} \text{ g cm}^{-2} \text{ h}^{-1}$ , respectively (**Figure 7**). The change in oxidation rate from bcc metal to fcc and hcp metals can be attributed to the increase in atomic packing fraction of different crystal structures and also the progressive decrease in the free energy of formation of iron, copper and zinc oxidation, respectively. The trend of oxidation rate from zinc towards iron may be both a combination of cations as well as anionic mobility. A marginal difference in thickness and structural changes in grain size and shape has been observed in the  $\text{Cu}_2\text{O}$  inner layer compared with  $\text{CuO}$  outer layer (**Figures 8 and 9**).

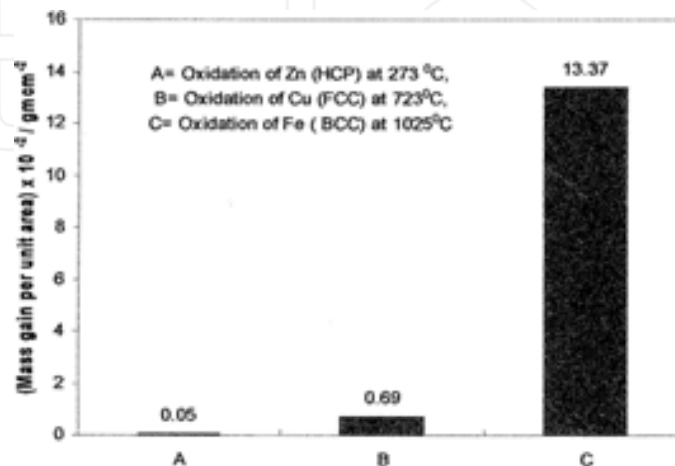


**Figure 7.** Oxidation behavior of Zn, Cu and Fe at high temperature ( $T=2/3 \text{ m.p.}$ ) in  $p=21.27 \text{ kPa}$  for 10 hours.

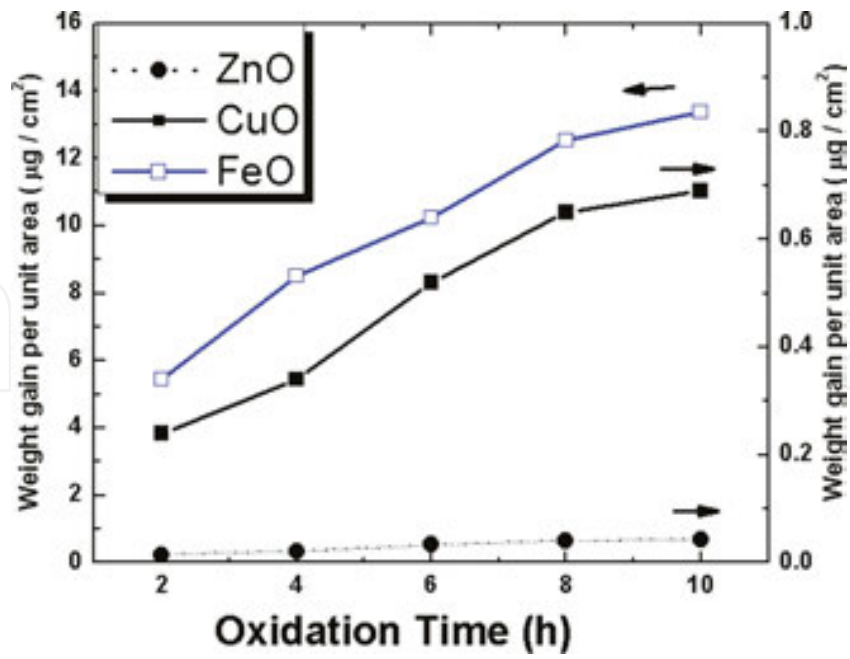


Figure 8. Oxidation kinetics of Fe, Cu and Zn layers under 21.27 kPa  $\text{O}_2$  at 1023 K, 723 K and 279 K.

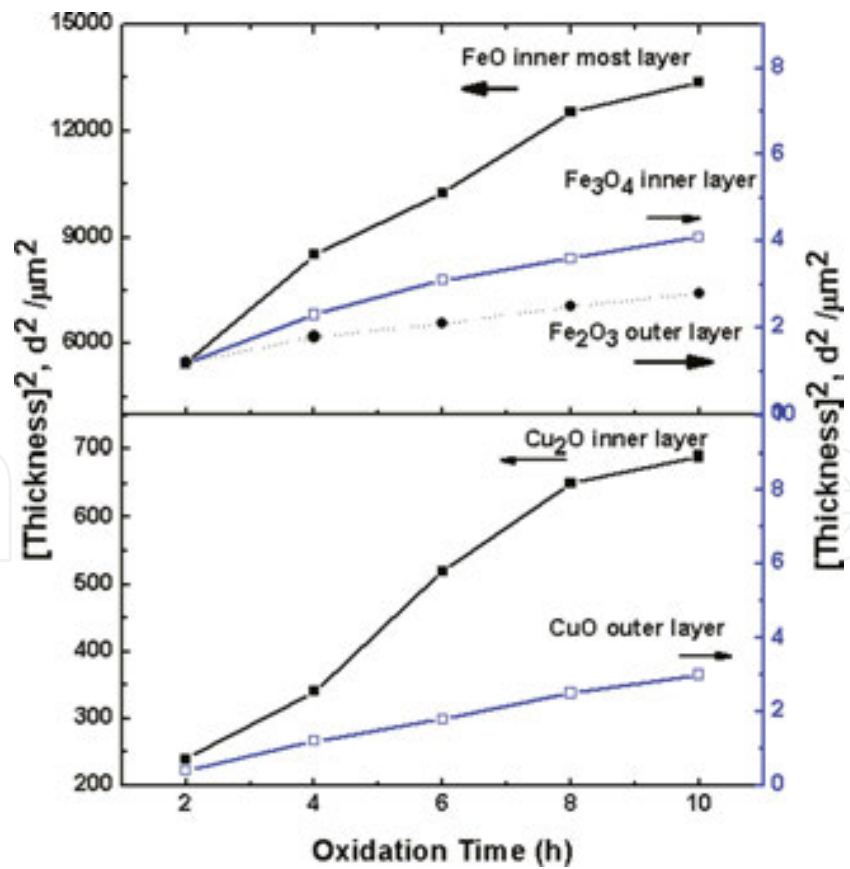
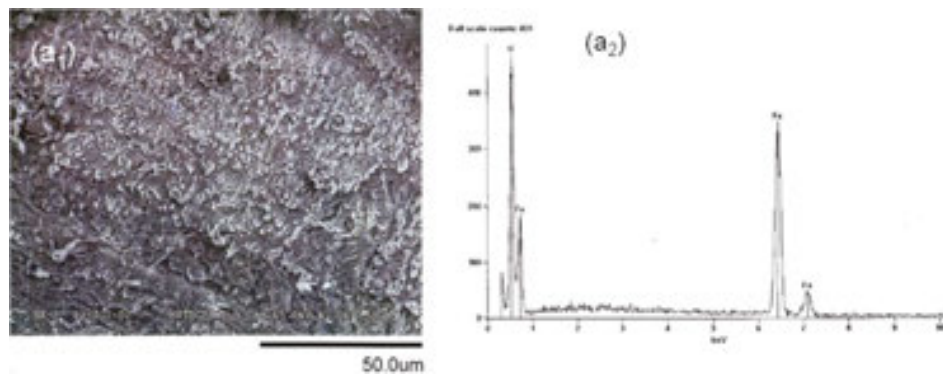
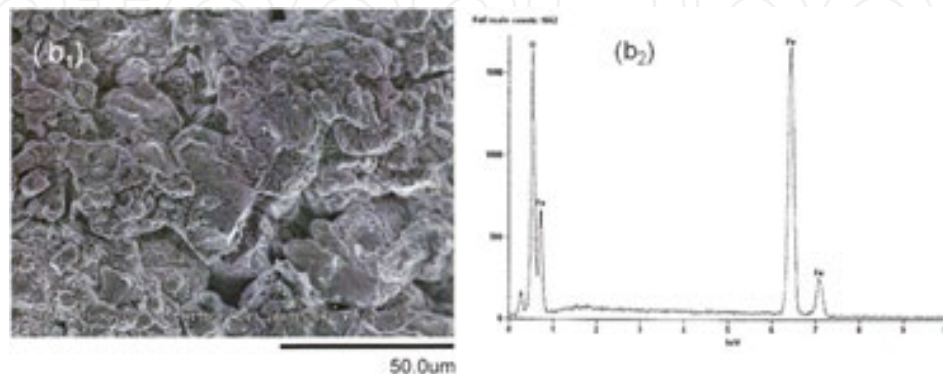


Figure 9. Scale of the oxidation layer of Fe and Cu layers under 21.27 kPa  $\text{O}_2$  at 1023 K and 723 K for 10 h.

The external scales of all the three samples are examined using SEM and EDS. The SEM micrograph of top oxide scale of pure iron and the corresponding EDX are shown in **Figure 10**. The top oxide scale on cooling to room temperature is found to be ballooned and separated from the metal substrate without any appearance of cracks. The observed ballooning of the scale can be attributed to the compressive stress generated within the scale as a result of higher volume of iron oxide compared to that of iron. The lower scale of the pure iron after unbounding from the base metal shows the creation of the holes and elongated cracks on the surface with irregular thickness of the surface morphology. Oxidized scale shows the rough microstructure with valleys around grain boundary. This indicates that the transport of cations along grain boundaries is still the dominant mechanism for outer scale growth. According to elemental composition, the outer layer consists of maximum oxygen than the inner layers with minimum amount at base ( $O_2$ ) content (upper surface area > lower surface area > base of the substrate). A common cause of such stress is the difference in thermal expansion coefficient of the oxide and metal. Oxide layer has low thermal expansion coefficient than the metal base component. If the corrosion rate is sufficiently low, then the oxide layer is always less than the critical thickness.



**Figure 10.** (a1) SEM micrograph of oxide scale on the substrate of pure iron after removal of top scale and (a2) corresponding EDX.



**Figure 11.** (b1) SEM micrographs of lower surface of the top scale of pure iron after detached from the base metal and (b2) corresponding EDX.

In the case of zinc the oxide layer is very thin and strongly adheres to the base metal with thickness less than 1  $\mu\text{m}$  (**Figure 11**). In the case of pure copper the scale does not spall but exhibits needle shape grains having different orientation on the top surface of the oxide scale. The pores are observed in the medium layer of the copper scale due to nonuniform thickness of layers that obey the parabolic rate law (**Figure 12**).

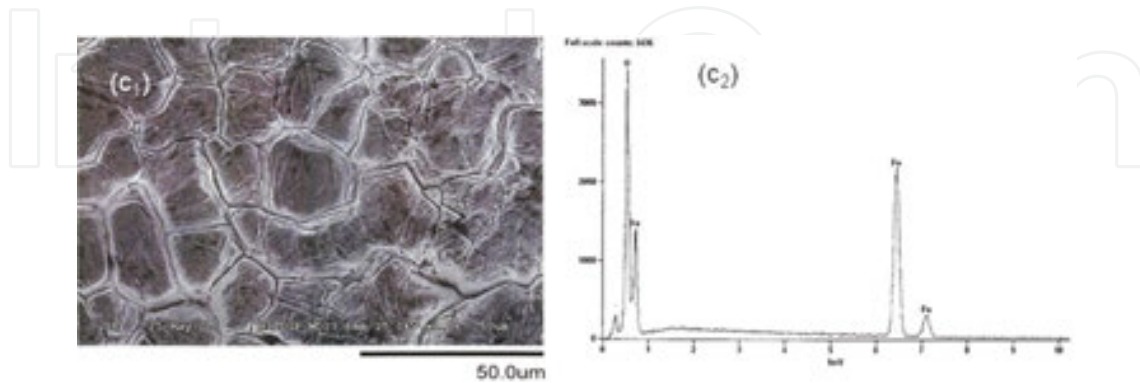


**Figure 12.** (c1) SEM micrograph of top oxide scale formed over pure iron (c2) and corresponding EDX.

## 6. Discussion on the mechanism of high-temperature oxidation

The degree of oxidation inhibited by voids depends on their continuity and location of oxide and their effective elimination by plastic deformation (**Figure 13**).

Oxidation rate decreases with decrease in grain size for pure iron and copper. As a result the stress caused by the conversion of  $\text{Fe}_3\text{O}_4$  to  $\text{Fe}_2\text{O}_3$  could create inner crystalline microcracks that simulate plastic behavior under differential contraction as well as diffusion paths during grain boundary diffusion areas (**Figure 13**). Grain shape and size highly influence the oxidation rate of pure metals at high temperature. Oxidation rate decreases with decrease in grain size up to a certain extent. Reaction and diffusion of metals in air influence the reaction kinetics of the oxidized layer of the metal (**Figure 14**). Kinetics of oxidation depends on both the metal and oxygen transport inward as well as outward diffusion in scale (**Figure 15**). The mechanism of compressive behavior of oxide scales on the metal surface that develop due to stresses and inner displacement that develops during oxidation process of metal (**Figure 16**). The oxidized grain size for Cu in comparison to grain boundary to bulk is shown in **Figure 17**. Interfacial reaction and transport mechanism of high-temperature oxidation through the oxide interface are shown in **Figure 18**. **Figure 19** displays the oxidized grain size of copper metal as a function of distance on oxide/metal interface. The illustration of grain boundary sliding and creation of cavity is shown in **Figure 20**. **Table 1** shows the summary of mechanism of surface-controlled oxidation mechanism. Finally, **Figure 21** explains graphical schematic presentation of oxidized scale on the pure metals such as Fe, Cu and Zn on high-temperature oxidation. The basic understanding on the influence of grain size and shape on the oxidation will derive knowledge for alloys' oxidation.

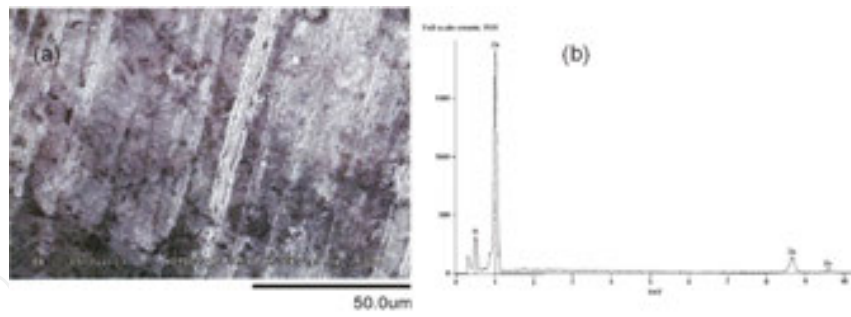


Figure 13. SEM micrograph of the top surface of the oxide scale of pure zinc (a) and corresponding EDX (b).

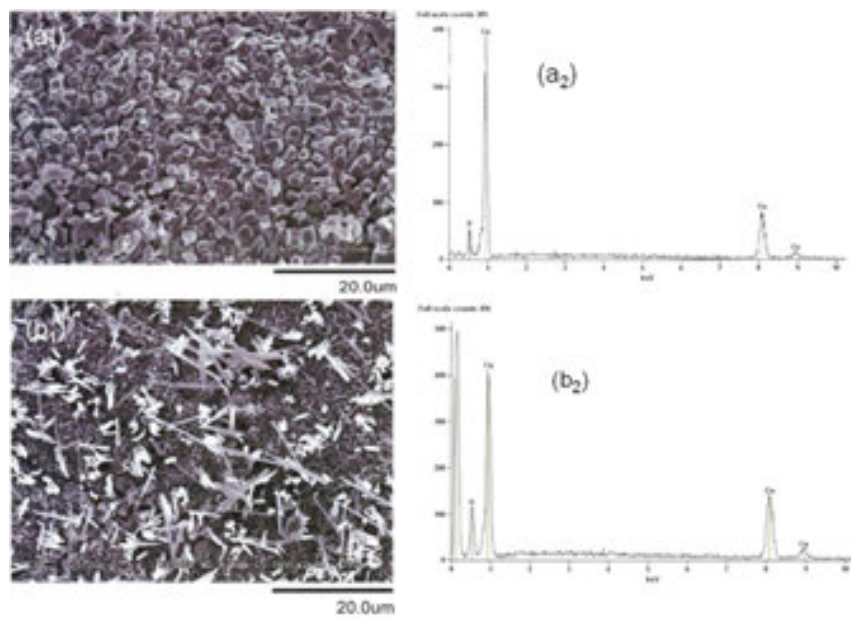


Figure 14. (a1) SEM micrograph of the top surface of the oxide scale of pure copper (a2) corresponding EDX. (b1) SEM micrograph of the inner oxide scale of copper (b2) corresponding EDX.

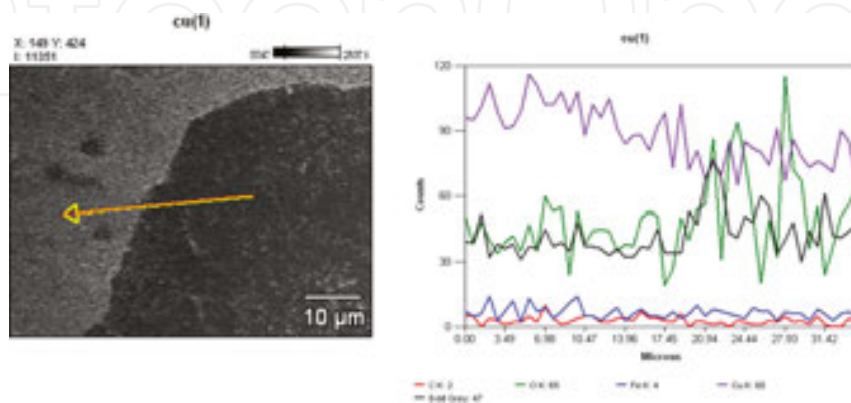


Figure 15. Line analysis of the oxide scale towards the base of the copper metal.

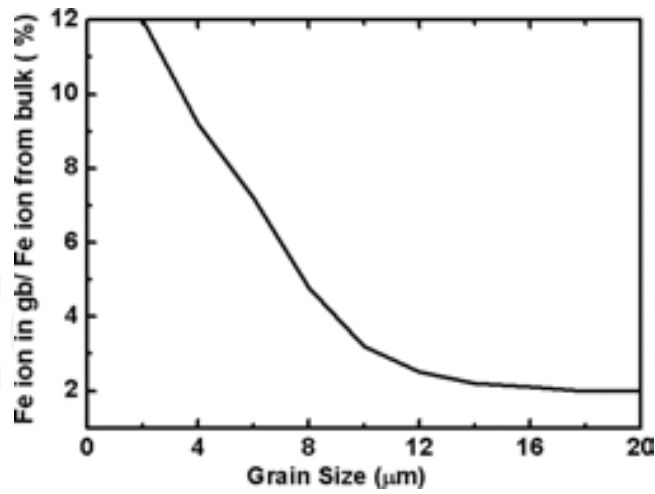


Figure 16. Oxidized grain size as a function of Fe ion in gb/Fe ion from bulk (pct).

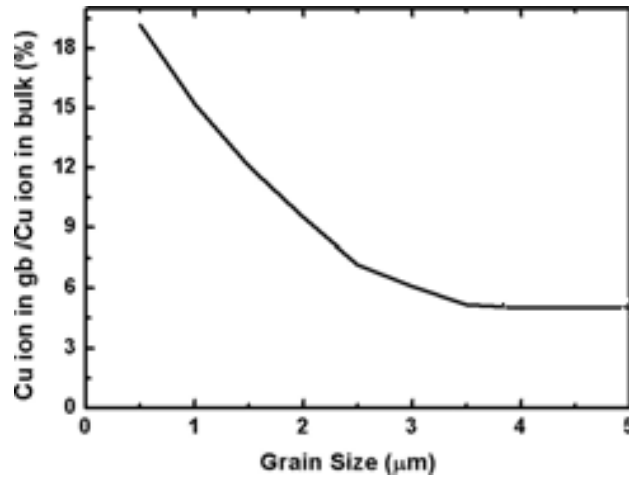


Figure 17. Oxidized grain size as a function of Cu ion in gb/Cu ion from bulk (pct).

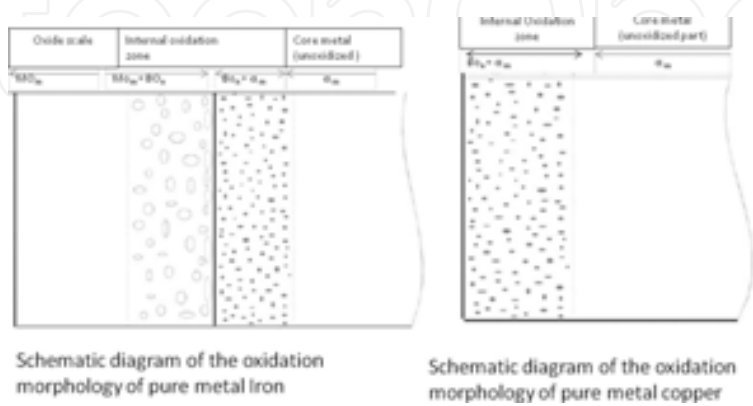
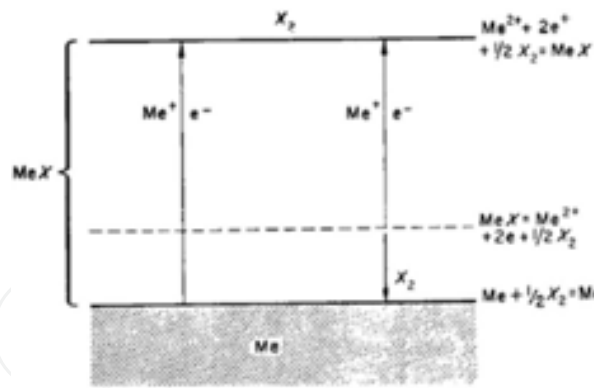
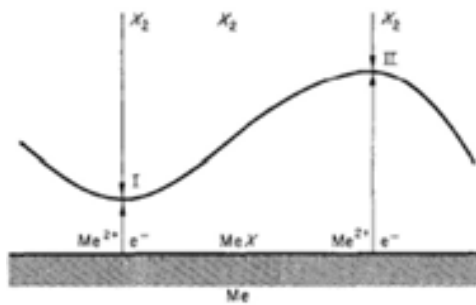


Figure 18. Interfacial reaction and transport processes for high-temperature oxidation mechanism.



Schematic process occurs during formation of double layer mono phase scale on a metal (Mrowec 1967).



Mechanism of formation of the initial layer of the reaction product on metal surface (sinusoidal curve).

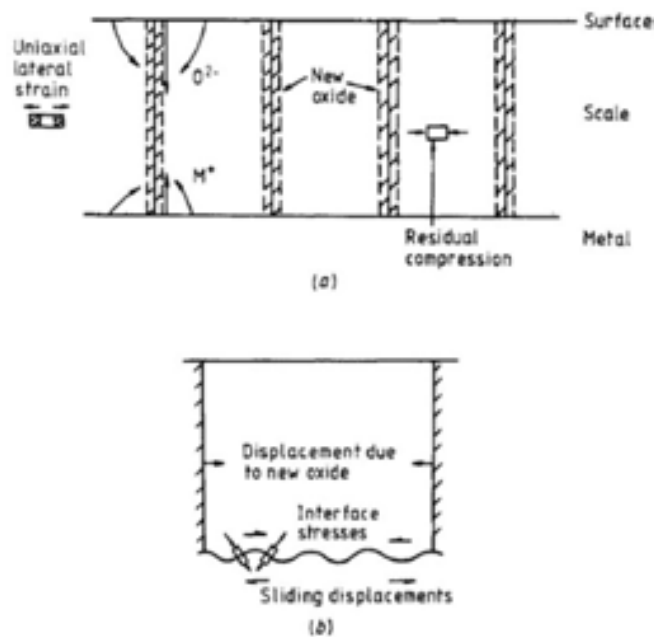
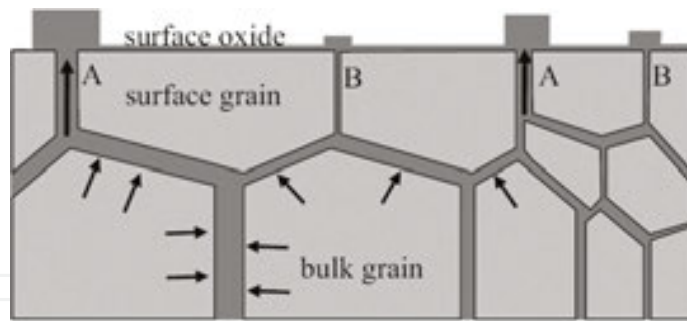


Figure 19. (a1) Compressive constraints on new oxide displacement at grain boundaries within the bulk scale. (b) The interface sliding displacement associated with oxide formation within the bulk scale (Evan et al.).



(c) Thickness of the grain boundary and grain size induces the mass transfer for the formation of oxide scale.

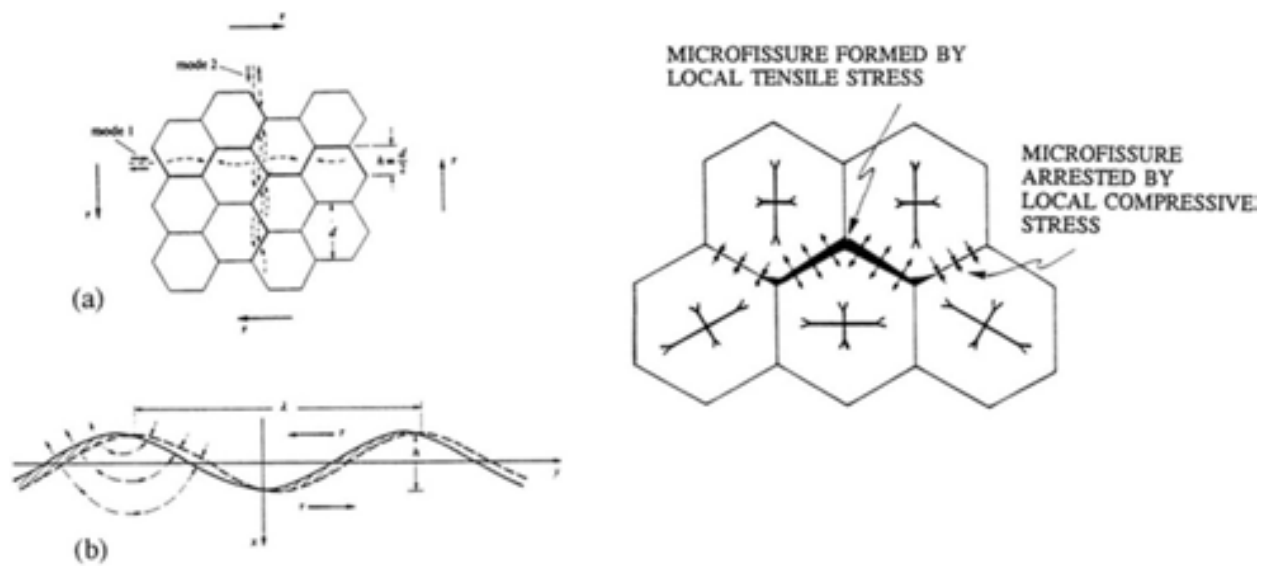


Figure 20. (a) Illustration of the grain boundary sliding, (b) the formation of cavity.

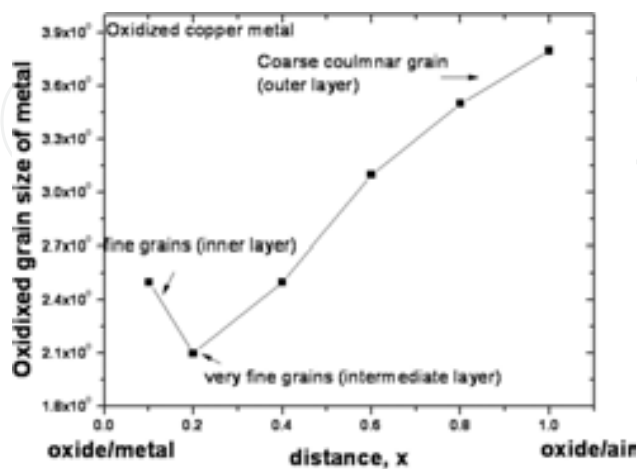


Figure 20. Oxidized grain size of the copper metal as a function of distance from the oxide/metal interface.

Initial premise	Electron concentration independent of oxide thickness	Electron concentration dependent on oxide thickness. Boltzmann distribution of electrons if field-producing ions are absorbed on the oxide surface	
Rate determining steps	Any surface reactions involving oxygen (e.g. $O + e^- \rightarrow O^-$ )	Most surface reactions involving ionized species except second ionization	Second ionization of surface species (e.g. $O^- + e^- \rightarrow O^{2-}$ )
$x$ = oxide thickness		$O^{2-}_{ads} \rightarrow O^{2-}_{oxide}$	
$Q$ = surface charge		$xQ/T \gg 1$	$xQ/T \ll 1$
$T$ = temperature (°K)			$xQ/T \gg 1$
$N$ = total no. of surface sites		$[O^{2-}] \ll N$	$[O] \ll N$
Kinetics	Linear	Parabolic	Linear
Cu reaction kinetics		Cu	
Fe reaction kinetics			Fe
Zn reaction kinetics			Zn
			Cubic
			Logarithmic

Table 1. Summary of the description of surface-controlled oxidation.

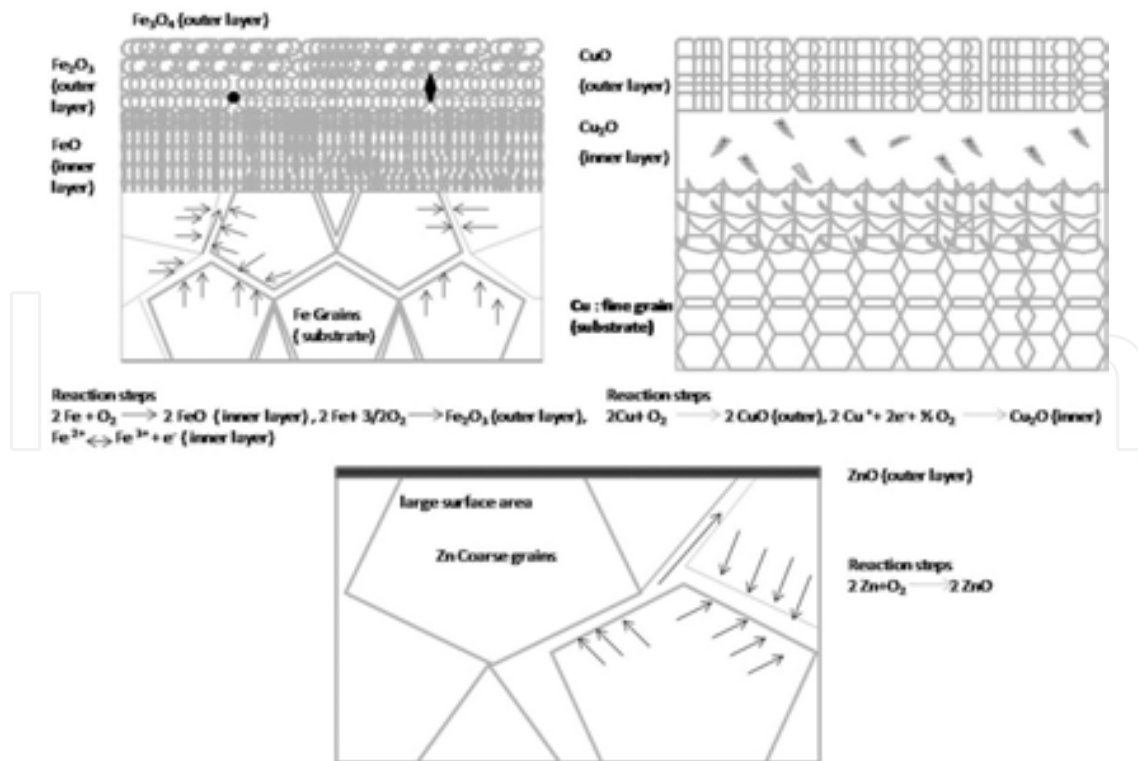


Figure 21. Schematic presentation of various oxide layers' formation on three pure metals.

## 7. Application of nanotechnology for the resistance of high-temperature corrosion in metals

Nanotechnology coating is emerged as the resistance to high-temperature corrosion in various metals from the last decade. Novel active anticorrosive pigments that consist of metal particles coated with a very thin layer of semiconducting titanium dioxide to protect the surface of metal at high-temperature operation. Nano TiO<sub>2</sub> is contributed towards the development of high corrosive resistance for materials with hydrophobic characteristics. Some polymer coatings such as polypyrrole nanocomposites with iron oxide Fe<sub>3</sub>O<sub>4</sub> are used in the corrosion protection of iron metal [25]. Also self-assembled nano phase coating is used for resistance of corrosion activity and promotes adhesion of inter surface bonding between metal and coating process [26]. Nano TiO<sub>2</sub> coating is used because it performs multifunctional activities such as anti UV radiation and anti-bacterial self-cleaning paints on the materials.

## 8. Conclusion

High-temperature oxidation of metals were studied based on the parameters such as specific crystal structure of metal, grain size and grain morphology of three different metals such as Cu, Fe and Zn. Fe and Cu show the formation of multilayers that obey the parabolic law however Zn metal deviates from the law. Scale morphology depends upon the initial crystal structure of the pure metals that leads towards the packing fraction of the material in lattice stage. Oxidation kinetics is also highly influenced by the structure of metals. The rate of oxidation decreased to a greater extent with change in the crystal structure from bcc → fcc → hcp. Change in crystal structure not only improved the oxidation resistance but also the scale adherence from bcc to hcp.

## Acknowledgements

Authors would like to thank Mr Sanjeeb Kumar Samal for his contribution regarding literature search for preparation of this article. Author is presently the assistant professor at Technical University of Liberec also with collaboration of this work with VUTs a.s. (research center) in Czech Republic.

## Author details

Sneha Samal

Address all correspondence to: [sneha.manjaree.samal@tul.cz](mailto:sneha.manjaree.samal@tul.cz)

The Centre for the Development of Engineering Research VÚTS, a.s., Liberec, Czech Republic

## References

- [1] R. E. Hummel. *Understanding materials science*. Springer-Verlag New York, Inc., USA, 2004, p. 36.
- [2] E. Opila. High temperature materials corrosion challenges for energy conversion technologies. *The electrochemical Society Interface*, Winter 2013, pp. 69–73.
- [3] S.C.Kung, Formation of a chromium-carbide conversion coating on silicon carbide , *Oxid. Met.* 1999, 5,516, pp. 191–203.
- [4] F. Cattant, D. Crusset, D. Feron. Corrosion issues in nuclear industry today. *Mater. Today* 2008, 11, 10.
- [5] D. Freon, D. D. Macdonald. *Prediction of long term corrosion behavior in nuclear waste system*, EFC series 36. Maney/Woodhead, London, 2003.
- [6] J. M. Boursier et al. A review of PWSCC, weldability, and thermal ageing of nickel weld metals in PWR primary water. Presented at EPRI International conference on PWSCC of alloy 600, Santa Anna Pubelo, USA, March 2005.
- [7] B. Riou et al. Issues in reactor pressure vessel materials. 2nd International Topical Meeting on High Temperature Reactor Technology, 2004.
- [8] A.Zahs, M.Spiegel, H.Grabhe, Chloridation and oxidation of iron, chromium, nickel and their alloys in chloridizing and oxidizing atmospheres at 400-700 °C, *Corr. Sc.* 2000, 42, 6, pp.1093–1122.
- [9] G. S. Was. *Fundamentals of Radiation Materials Science: Metals and alloys*. Springer Verlag, 2007, The materials information society. ASM international, Materials Park, OH 44073-0002, ISBN: 978-3-540-49471-3.
- [10] M. Rühle, U. Salzberger and E.Schumann. High resolution transmission microscopy of metal/metal oxide interfaces. In *microscopy of oxidation 2*. Eds. S.B.Newcomb and M.J. Bennett, London, Uh, The institute of Materials, 1993, p.2.
- [11] D. R. Gaskell. *Introduction the thermodynamics of materials*, 3rd edn, Taylor and Francis, Washington, DC, 1995.
- [12] M. Hillert. The uses of Gibbs free energy–composition diagrams. In *Lectures on the Theory of Phase Transformations*, 2nd edn., H. I. Aaronson (Ed.), The Minerals, Metals and Materials Society, Warrendale, PA, 1999.
- [13] D. M. Smyth. *The defect chemistry of metal oxides*. Oxford University Press, Oxford, 2000.
- [14] R.J.Hussey and M.J.Graham, The influence of reactive-element coatings on the high-temperature oxidation of pure Cr and high Cr content alloys, *Oxid. Met.* 1996, 46, 3/4, pp. 349–374.

- [15] A.S.Khanna. Introduction to high temperature oxidation and corrosion. ASM International. ] S.C.Kung, Formation of a chromium-carbide conversion coating on silicon carbide , *Oxid. Met.* 1999, 5,516, pp. 191-203.ISBN:0-87170-762-4. The materials information society.
- [16] C.M.Cotell, G.J.Yurek, R.J.Hussey, D.F.Mitchell, M.J.Graham. The influence of grain boundary segregation of Y in Cr<sub>2</sub>O<sub>3</sub> on the oxidation of metals. 1990, 34,3pp.173–200.
- [17] R. A. Perkins, G. H. Meier. Acoustic emission studies of high temperature oxidation. In *High Temperature Materials Chemistry*, Z. A. Munir, D. Cubicciotti (Eds.), Electrochemical Society, New York, NY, 1983, p. 176.
- [18] N.Birks, G.Meier and F.Petit. Introduction to the high temperature oxidation of metals, 2nd eds, The Cambridge university press.
- [19] R Mishra, R. Balasubramaniam. Effect of nanocrystalline grain size on the electrochemical and corrosion behaviour of nickel. *Corros. Sci.*, 2004, 46, 3019–3029.
- [20] M. Kending, M. Hon, L. Warren. Smart corrosion inhibiting coating. *Progr. Org. Coat.* 2003, 47, 183–189.
- [21] P. Kofstad. *High Temperature Corrosion*. Elsevier Applied Science Publishers, Ltd, New York, 1988.
- [22] H. E. Evans. In *Cyclic oxidation of high temperature materials*. M. Schutze, W. J. Quadackers (Eds.), IOM communications, London, 1999, p. 437.
- [23] Pin Lu, Engelhardt George R., B. Kursten, D. D. Macdonald. The kinetics of nucleation of metastable pits on metal surfaces: The point defect model and its optimization on data obtained on stainless steel, carbon steel, iron, aluminium, alloy 22. *J. Electrochem. Soc.*. 2016 163 (5) C156-C163.
- [24] V. S. Saji, Joice Thomas. Nanomaterials for corrosion control. *Curr. Sci.* 2007, 92, 1.
- [25] H. S. Nalwa (Ed.). *Handbook of nanostructured materials and nanotechnology*, Vol. 1, Academic Press, San Diego, 2000.
- [26] A. G. Evans, J. W. Hutchinson, and Y. Wei, Interface adhesion: effects of plasticity and segregation, *Acta mater.* Vol. 47, Nos 15, pp. 4093–4113, 1999.
- [27] S Samal and S K Mitra. Influence of grain shape, size , grain boundary diffusion on high-temperature oxidation of pure metal Fe, Cu and Zn. *Metall. Mat. Transc. A* 2015, 46A, pp. 3324–3332.

